Zeeman Scanning of Persistent Spectral Holes in Amorphous Hosts. Application to the R_1 Line of $[Cr(NCS)_6]^{3-}$ in Glycerol

Hans Riesen*

School of Chemistry, University College, The University of New South Wales, Australian Defence Force Academy, Canberra, ACT 2600, Australia

Received: December 7, 1999; In Final Form: February 28, 2000

Persistent spectral holes in amorphous systems can remain sharp and may display a linear shift upon the variation of the external magnetic field when they are burned in high fields. Experiments were performed on the R line of $[Cr(NCS)_6]^{3-}$ in glycerol at 4.2 K. When the spectral hole is burned in a field of 3.2 T it displays a linear shift of 26.4 GHz/T upon the variation of the magnetic field strength from 2.8 to 3.6 T. The shift corresponds to an average excited-state *g*-value of 2.17. The broadening of the hole implies an upper limit of the anisotropy and/or strain of the excited *g*-value of ≈15%. The linear shift can be used to read out the spectral hole by sweeping the magnetic field.

1. Introduction

Optical excitations in the solid state are subject to inhomogeneous broadening which is caused by the variation of local fields in the vicinity of the chromophores.[1−4] The inhomogeneous broadening is particularly severe in amorphous systems. Laser techniques such as spectral hole-burning can overcome this broadening and it is often possible to increase the spectral resolution by a factor of $>10^5$.

Persistent spectral hole-burning is an ubiquitous phenomenon in optical transitions of chromophores embedded in amorphous systems.[1]

A subset of chromophores may undergo some photophysical or photochemical changes upon its selective excitation by laser light.

Persistent spectral hole-burning in amorphous systems has been applied to study a wide range of topics such as homogeneous line widths,[2] zero field splittings (ZFSs),[5] vibrational sidelines,[6] the interaction of dye molecules with DNA,[7] spectral diffusion,[8] Stark effects in electronic origins,[9] and energy transfer in biological systems.[10]

Also, external magnetic fields have been applied to persistent spectral holes in amorphous systems.[11] Unfortunately, the information which can be derived from these latter experiments is usually obscured by severe and featureless hole broadening upon the application of an external magnetic field.

In the present work it is shown that Zeeman experiments on spectral holes in amorphous systems can be very informative when the hole is burned in a high magnetic field. For example, holes in particular transitions, such as the $^4A_2 \rightarrow {}^2E$ excitations in chromium(III), can remain sharp and display a linear shift when the external magnetic field is varied. The linear shift facilitates the read out of spectral holes by sweeping the magnetic field.

2. Experimental Section

Samples were prepared by dissolving $K_3Cr(NCS)_6 \cdot 4H_2O$ (Pfaltz&Bauer) in glycerol (Aldrich). The solution forms a good glass upon rapid cooling in a quartz cell of 8 mm diameter and 1 mm path length. The samples were cooled either by the flow tube technique[12] or in a cryomagnet (BOC 5T).

Nonselective luminescence spectra were excited by a 1 mW green He−Ne laser (543.5 nm). For selective spectroscopy an Ar^+ laser (Spectra Physics 171) pumped single frequency Ti:sapphire ring laser (Schwartz Electrooptics) was used. For the high-resolution hole-burning experiments the Ti:sapphire laser was tuned discontinuously by tilting the intracavity étalon with a galvanometer. The laser then mode hops in steps of ≈245 MHz which corresponds to the longitudinal mode spacing. The frequency of the laser was tracked by a temperature stabilized and sealed confocal scanning Fabry−Pérot interferometer (Burleigh CFT-25P, 3 GHz free spectral range). For lower resolution hole-burning experiments the intracavity étalon was removed and the laser tuned with an effective line width of ≈10 GHz by a three-plate birefringent assembly.

The luminescence was dispersed by a Spex 1404 0.85 m double monochromator and detected by a red sensitive RCA-31034 photomultiplier. For resonant experiments the laser light was passed through the same chopper blade as the luminescence but with a phase shift of 180°.

The magnetic field was applied along the propagation direction of the laser beam i.e., the electric vector of the exciting laser light was perpendicular to the magnetic field direction, $\mathbf{E} \perp \mathbf{B}$.

3. Results and Discussion

Figure 1 shows the nonselectively excited and monitored luminescence and excitation spectra of $[Cr(NCS)_6]^{3-}$ in glycerol at 12 K in the region of the $^4A_2 \rightarrow {}^2E$ transition. Luminescence occurs predominantly from the lower lying component of the ^2E state at 12 K ,whereas the two R lines carry comparable intensity in excitation. Thus, the Stokes shift of 40 cm^{-1} between the maxima of the origin in luminescence and excitation is due to the R line splitting. Hence the two intense sidelines at 238 and 475 cm^{-1} show comparable integrated intensities relative to the electronic origins in excitation and luminescence. An analysis of vibrational sidelines in the luminescence spectrum of crystalline $K_3[Cr(NCS)_6] \cdot 4H_2O$ has been reported in ref 13.

* Corresponding author. E-mail: h-riesen@adfa.edu.au. Fax: ++61 (0)2 6268 8017.

10.1021/jp994290l CCC: $19.00
Published on Web 05/23/2000

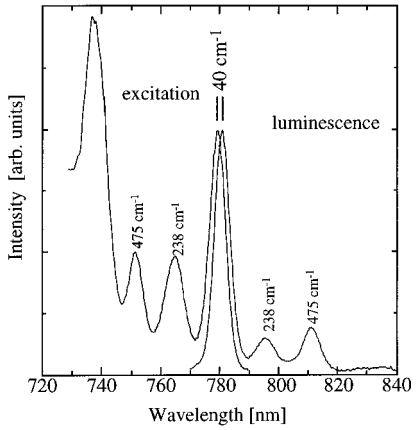

Figure 1. Nonselective luminescence and excitation spectra of $[Cr(NCS)_6]^{3-}$ in glycerol at 12 K in the region of the $^4A_2 \rightarrow {}^2E$ transition.

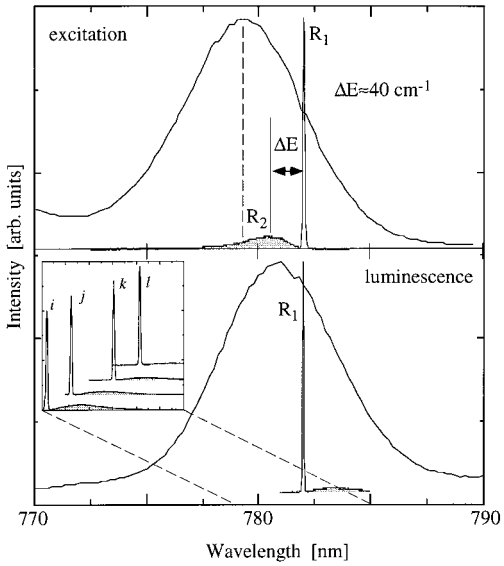

Figure 2. Resonantly narrowed excitation and luminescence spectra of $[Cr(NCS)_6]^{3-}$ in glycerol at 20 K in the region of the electronic origins. The spectra were monitored and excited at 782 nm, respectively. The inset shows resonantly narrowed luminescence spectra excited at i, 779.20 nm; j, 780.25 nm; k, 782.05 nm; and l, 783.15 nm.

Following that analysis the sideline at 238 cm^{-1} can be assigned to overlapping bands of Cr−N−CS bending modes with T_{1u} and T_{2u} symmetry. The sideline at 475 cm^{-1} is interpreted as a T_{2u} N−C−S bending mode. There appears to be another electronic origin at ≈737 nm which is most likely due to a component of the $^4A_2 \rightarrow {}^2T_1$ transition.

In Figure 2 resonantly narrowed luminescence and excitation spectra are shown in the region of the R lines. The resonantly narrowed line is accompanied by a broad feature both in luminescence and excitation. As is illustrated in the inset of Figure 2 the intensity of this broader feature is strongly dependent on the wavelength of excitation for the narrowed luminescence spectra. In particular, its intensity decreases with excitation at longer wavelengths. This excludes the possibility that this feature is due to a phonon sideline in accord with the fact that the coupling of R lines in chromium(III) systems to low-frequency phonons is usually very weak. It is then safe to assign the broad feature to the second R line. The shorter the wavelength of excitation within the inhomogeneous distribution the more likely it becomes that some complexes are excited via the R_2 line. Thus, the contribution from the resonantly excited R_2 line to the narrowed feature increases with decreasing

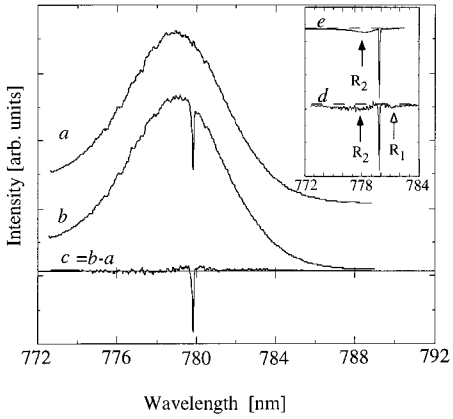

Figure 3. Spectral hole burning of the R lines in $[Cr(NCS)_6]^{3-}$/glycerol at 15 K. The excitation spectrum is shown (a) before and (b) after burning a hole at 779.85 nm for 600 s with a laser power density of ≈1 W/cm^2. A narrowed excitation spectrum e is shown in the inset in comparison with the hole-burning spectrum d from which (1/90)a has been subtracted to correct for the antihole absorbance by the photoproduct.

wavelength and the intensity of the corresponding broader R_1 feature at longer wavelength increases. The ratio of luminescence from the narrowed R_2 line and the broad R_1 line $I(R_2)/I(R_1)$ can be calculated by eq 1 which is based on the Boltzmann distribution and the experimental line shape $f(\Delta E)$ of the broad R_1 line feature. ΔE denotes the energy difference to the resonant R_2 line.

$$I(R_2)/I(R_1) = \frac{\int_{-\infty}^{\infty} f(\Delta E) e^{-\Delta E/kT}/(1 + e^{-\Delta E/kT}) d\Delta E}{\int_{-\infty}^{\infty} f(\Delta E)/(1 + e^{-\Delta E/kT}) d\Delta E} \quad (1)$$

For example, for the narrowed luminescence spectrum i in the inset of Figure 2 a ratio of $I(R_2)/I(R_1) = 0.36$ is calculated for resonant R_2 excitation at 20 K. The experimental ratio is ≈0.75. This implies that the narrowed feature in trace i consists of ≈50% contributions from both the R_1 and the R_2 line. This is in accord with the fact that the excitation wavelength for trace i is approximately at the peak maximum of the nonselective excitation spectrum.

As is indicated in the narrowed excitation spectrum in Figure 2, the broad R_2 feature is separated from the resonant line by 40 cm^{-1} reflecting the Stokes shift observed in the nonselective spectroscopy illustrated in Figure 1. It appears that although there is a substantial variation of the R line splitting causing the actual width of the broader feature there is a degree of correlation between the two lines within the inhomogeneous distribution. For example, in the narrowed excitation spectrum of Figure 2 the width of the broad feature is somewhat smaller than the total inhomogeneous width and its maximum is at longer wavelength in comparison with the nonselective spectrum. The width of the narrowed line is instrumentally limited by the resolution of the monochromator in the spectra shown in Figure 2. The homogeneous line width is substantially narrower even at the experimental temperature of 20 K.

Figure 3 displays a spectral hole-burning experiment measured at low resolution. From the difference spectrum c it follows that the photoproduct is within the inhomogeneous distribution which indicates that a nonphotochemical hole-burning mechanism is effective. The inset compares a narrowed excitation spectrum e with the hole-burning spectrum d which has been corrected for the antihole spectrum of the photoproduct. The broader hole at shorter wavelength is due to the R_2 line.

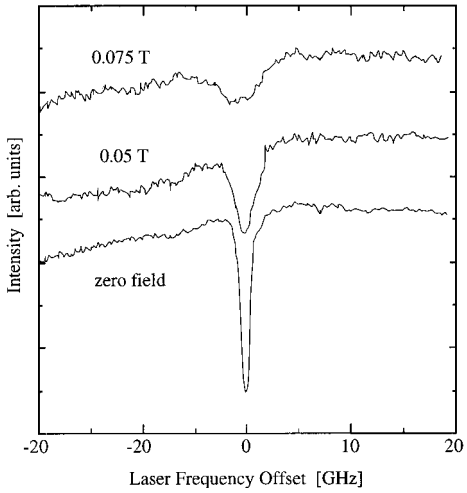

Figure 4. Zeeman effect on a spectral hole burned at 4.2 K into the R_1 line of $[Cr(NCS)_6]^{3-}$/glycerol at 781.8 nm.

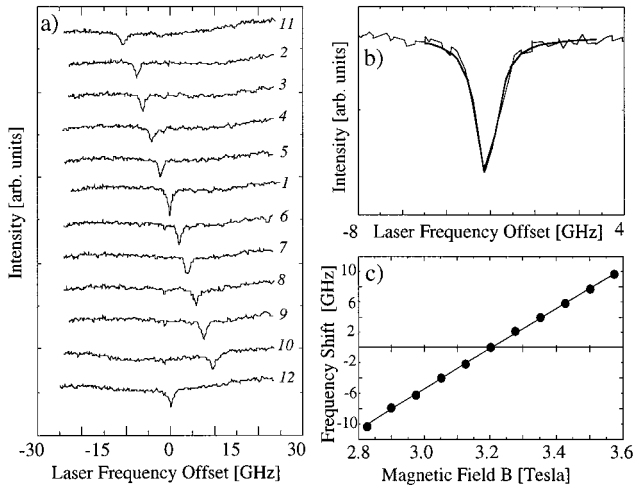

Figure 5. (a) Zeeman effect on a spectral hole burned into the R line of the $[Cr(NCS)_6]^{3-}$/glycerol at 781.8 nm and 4.2 K in a field of 3.2 T. Trace 1 shows the initial hole. The field was then varied in the range of 2.83−3.58 T in the following sequence; 2, 2.90 T; 3, 2.98 T; 4, 3.05 T; 5, 3.13 T; 6, 3.28 T; 7, 3.35 T; 8, 3.43 T; 9, 3.50 T; 10, 3.58 T; 11, 2.83 T; 12, 3.2 T. (b) A fit to Lorentzian line shape of the hole in trace 5. (c) The shift of the spectral hole as a function of the field (data points) in comparison with a linear least-squares fit (solid line).

However, at the burn wavelength some chromophores are excited also via the R_2 line causing a shallower broad side hole at longer wavelengths due to the R_1 line.

Figure 4 shows the effect of an external magnetic field on a spectral hole burned at 781.8 nm in zero field. Upon the application of a relatively low magnetic field of 0.075 T substantial hole broadening occurs.

The Zeeman effect is drastically different when the spectral hole is burned in a high magnetic field and the field strength is subsequently varied. This is shown in Figure 5. The hole broadening is relatively small over a significant variation of the field and a linear hole shift of 26.4 GHz/T is observed.

The zero field splitting and the Zeeman effect in the $^4A_2$ ground state can be described by following spin Hamiltonian

$$H = D[S_z^2\text{-}1/3S(S+1)] + E(S_x^2 - S_y^2) + \mu_B \mathbf{g}\cdot\mathbf{B}\cdot\mathbf{S} \quad (2)$$

For the case of low symmetry ($<C_{2v}$), the axes of the **g**-tensor do not necessarily coincide with the principal axes of the zero

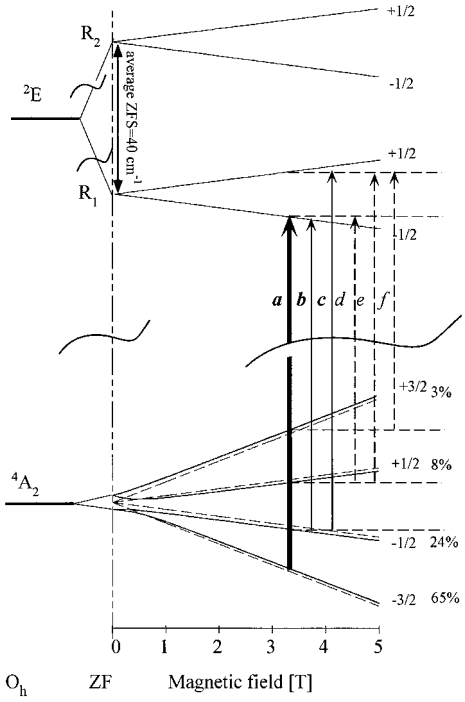

Figure 6. Schematic diagram of the relevant $^4A_2 \rightarrow {}^2E$ transitions in an external magnetic field. The populations of the $^4A_2$ spin levels are indicated for a field of 3.2 T and a temperature of 4.2 K. The Zeeman effect in the ground state is shown without a (dashed line) ZFS and with (solid line) $D = E = 0.1$ cm^{-1} and $\Theta = 45°$.

field splitting (ZFS) described by D and E. However, in a first-order approximation the $[Cr(NCS)_6]^{3-}$ complex is close to octahedral.

From measurements of dynamic frequency shifts in the EPR of $[Cr(NCS)_6]^{3-}$ in methanol/ethanol an isotropic ground-state g-value of 1.98 and a parameter $\Delta = (2/3D^2 + 2E^2)^{1/2} = 4$ GHz was deduced.[14] For an isotropic g-value matrix (3) describes the Zeeman effect and the ZFS for the $^4A_2$ ground state where μ_B is the Bohr magneton.

	$^3/_2$	$^1/_2$	$-^1/_2$	$-^3/_2$
$^3/_2$	$D + (3/2)\times$ $g\mu_B B_z$	$(\sqrt{3}/2)g\mu_B\times$ $(B_x - iB_y)$	E	0
$^1/_2$	$(\sqrt{3}/2)g\mu_B\times$ $(B_x + iB_y)$	$-D +$ $^1/_2 g\mu_B B_z$	$g\mu_B\times$ $(B_x - iB_y)$	E
$-^1/_2$	E	$g\mu_B$ $(B_x + iB_y)$	$-D -$ $^1/_2 g\mu_B B_z$	$(\sqrt{3}/2)g\mu_B\times$ $(B_x - iB_y)$
$-^3/_2$	0	E	$(\sqrt{3}/2)g\mu_B\times$ $(B_x + iB_y)$	$D -$ $3/2 g\mu_B B_z$

(3)

Both ^2E components split into their $\pm^1/_2$ spin components in a magnetic field. A schematic diagram summarizing the relevant levels and transitions is shown in Figure 6.

Hole-burning in *zero field* involves both transitions from the $^4A_2$ multiplet to the lower lying ^2E component, i.e., $|\pm^3/_2(^4A_2)\rangle \rightarrow |\pm^1/_2\rangle$ and $|\pm^1/_2(^4A_2)\rangle \rightarrow |\pm^1/_2\rangle$. The ZFS splitting of the $^4A_2$ ground state (described by the parameters D and E) varies within the inhomogeneous distribution.[15] When a magnetic field is applied, the four spin levels of the ground state and the two spin levels of the lower component of the ^2E excited state split and the hole rapidly broadens because of the distribution of the ZFS and the random orientation of the chromophores with

respect to the external magnetic field. The following parameters are required to model this broadening; the average ZFS of the $^4A_2$ ground state and its distribution, the *g*-values of the ground and the excited state and their distributions and the two transition probabilities for the transitions $|\pm^3/_2(^4A_2)\rangle \rightarrow |\pm^1/_2\rangle$ and $|\pm^1/_2(^4A_2)\rangle \rightarrow |\pm^1/_2\rangle$. The data can be modeled by a simulation which averages the Zeeman effect over all angles between the axes of the **g**-tensor and the external magnetic field.[11] The broadening is relatively uncharacteristic, and thus, an accurate evaluation of parameters is difficult.

The analysis is somewhat simplified when the hole is burned in a high magnetic field. In particular, the Zeeman effect becomes independent of the ZFS.

With random orientation of the chromophores in the amorphous system with respect to the magnetic field, the eigenvectors of the $^4A_2$ ground state will be of the general form $|M_S'\rangle = c_1|^3/_2\rangle + c_2|^1/_2\rangle + c_3|-^1/_2\rangle + c_4|-^3/_2\rangle$. In a field of 3.2 T and zero-field splitting parameters of $D \approx 0.1$ cm^{-1}, $E \approx 0.1$ cm^{-1}, the orientational average of the squares of the four coefficients is close to 0.25. Hence the six possible transitions $|M_S'(^4A_2)\rangle \rightarrow |M_s(^2E)\rangle$ with $\Delta M_s = 0, \pm 1$ have comparable total transition probabilities. However, the Boltzmann populations of the spin levels in the ground state vary substantially in a field of 3.2 T. At 4.2 K and 3.2 T the populations of the $|-^3/_2'\rangle$, $|-^1/_2'\rangle$, $|+^1/_2'\rangle$, And $|+^3/_2'\rangle$ ground-state spin levels are about 65%, 24%, 8%, and 3%, respectively.

Because the inhomogeneous width is much larger than the Zeeman splitting of the levels the six transitions $|M_S'(^4A_2)\rangle \rightarrow |M_s(^2E)\rangle$ ($\Delta M_s = 0,\pm 1$) are accidentally degenerate for six subsets of chromophores that is to say there are chromium(III) complexes which have any of the six transitions in resonance with the laser frequency. After the hole is burned and the magnetic field is varied, this accidental degeneracy is lifted.

Each of the six resonant hole contributions is accompanied by five side holes due to the other transitions. However, these side holes are broad because of the spread of the ZFS within the inhomogeneous distribution. Since the inhomogeneous width is much larger than the ZFS, the hole-burning experiment is only energy selective but not site selective. For example, the hole contribution by the transition a $|-^3/_2'(^4A_2)\rangle \rightarrow |-^1/_2(^2E)\rangle$ will involve basically chromophores with the entire range of the ZFS.

Hole-burning spectroscopy is a "tandem" two-photon process. The first photon is used to burn the hole and the second photon is used for the read out. In the burn process the time dependence of the depletion of the six subsets of chromophores which have one of the $|M_S'(^4A_2)\rangle \rightarrow |M_s(^2E)\rangle$ ($\Delta M_s = 0,\pm 1$) transitions in resonance with the laser frequency will be dependent on the population of the ground state spin level and is given approximately by following first-order kinetics.

$$\text{depletion of subset } i = S(1 - \exp(-cP(M_S')t) \qquad (4)$$

In eq 4 *S* is the saturation depletion, $P(M_S')$ is the Boltzmann population of the spin level M_S' and *c* is a constant which depends on the absorption cross section, the concentration of chromophores and the power density of the laser radiation.[16]

When shallow holes are burned the depletion of the six subset of chromophores is approximately proportional to their Boltzmann population factors $P(M_S')$ of the ground-state spin level involved in the transition. When the holes are read out the Boltzmann population has to be taken into account for a second time. Thus, for shallow holes the contribution of a transition $|M_S'(^4A_2)\rangle \rightarrow |M_s(^2E)\rangle$ to the hole is approximately proportional to $(P(M_S'))^2$. It follows then that for shallow holes at 4.2 K and 3.2 T the $|-^3/_2'\rangle \rightarrow |-^1/_2)\rangle$ transition dominates the hole-burning spectrum.

In the high field limit the shifts of the ground-state spin-levels described by matrix (3) become independent of the ZFS. This is illustrated in Figure 6 which compares the Zeeman effect of the $^4A_2$ multiplet with and without a ZFS. For a change of the magnetic field of ΔB the ground-state spin levels $-^3/_2$ and $-^1/_2$ shift by $-^3/_2 g\mu_B \Delta B$ and $-^1/_2 g\mu_B \Delta B$, respectively,when the Zeeman energy becomes much larger than D and E. In the present system the ZFS is on the order of 3−10 GHz. The high field limit is thus reached when $B > 1$ T. Thus, for the entire range of chromophores with varying ZFS which are probed in the hole-burning experiment the hole shift caused by the energy change of the ground-state spin level becomes independent of the ZFS.

The excited-state spin levels $+^1/_2$ and $-^1/_2$ shift by $\pm^1/_2\mu_B[(g_x\Delta B_x)^2 + g_y\Delta B_y)^2 + (g_z\Delta B_z)^2]^{1/2}$. Thus, a transition $|M_S'(^4A_2)\rangle \rightarrow |M_s(^2E)\rangle$ of a complex with a particular orientation with respect to the external magnetic field **B** displays following shift when the field is varied:

$$\Delta E_i = M_s(^2E)\mu_B[(g_x\Delta B_x)^2 + (g_y\Delta B_y)^2 + (g_z\Delta B_z)^2]^{1/2} - M_S'(^4A_2)g\mu_B\Delta B \qquad (5)$$

The *orientational* average of the shift of transition i, $\Delta_{av}E_i$, is given by

$$\Delta_{av}E_i = \mu_B\Delta B[M_s(^2E)g_{ex}^{av} - M_S'(^4A_2)g] \qquad (6)$$

where we define the average *g*-value of the excited-state g_{ex}^{av} as

$$g_{ex}^{av} = \frac{1}{4\pi}\int_0^{2\pi}\int_0^{\pi}(g_x^2\sin^2\theta\cos^2\varphi + g_y^2\sin^2\theta\sin^2\varphi + g_z^2\cos^2\theta)^{1/2}\sin\theta\,d\theta\,d\varphi \qquad (7)$$

For example, the hole due to the $|-^3/_2'(^4A_2)\rangle \rightarrow |-^1/_2(^2E)\rangle$ transition shifts by

$$\Delta_{av}E_a = {}^1/_2\mu_B\Delta B(3g - g_{ex}^{av}) \qquad (8)$$

The integral in eq 7 can be solved for the axial case $g_x = g_y$

$$g_{ex}^{av}(g_x{=}g_y) = {}^1/_2(g_z + g_x)^2/(g_z^2 - g_x^2)^{1/2}\text{arctanh}[(g_z^2 - g_x^2)^{1/2}/g_z] \qquad (9)$$

The general anisotropic case can be approximated using a Taylor expansion around $x = y{=}1$ where *x* and *y* are given by

$$g_x = x^{1/2}g_z, \quad g_y = y^{1/2}g_z \qquad (10)$$

$$g_{ex}^{av} \cong g_z[1 + {}^1/_6\{(x-1) + (y-1)\} - 1/40\{(x-1)^2 + {}^2/_3(x-1)(y-1) + (y-1)^2\} + 1/112\{(x-1)^3 + {}^2/_5(x-1)^2(y-1) + {}^2/_5(x-1)(y-1)^2 + (y-1)^3\} + ...] \qquad (11)$$

We note here that for anisotropies of <30% it is sufficient to use the first three terms of the Taylor expansion (including quadratic terms). For example, when $g_x = 1.52$, $g_y = 2.82$, and $g_z = 2.17$ we obtain $g_{ex}^{av} \approx 2.23$ which compares favorably with the exact integral of $g_{ex}^{av} = 2.21$ obtained by numerical integration.

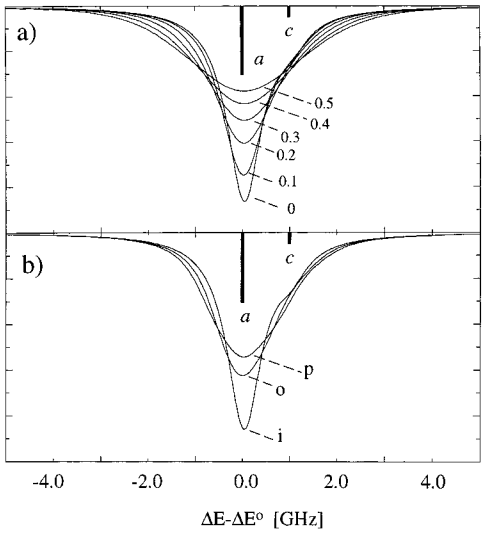

Figure 7. Simulation of the broadening due to strain or anisotropy of the excited-state *g*-value of a hole burned in a high magnetic field. The transitions a and c were weighed with $P(M_S')^2$. The calculations were performed for $\Delta B = 0.38$ T. The initial hole was described by a Lorentzian of $\Gamma_{initial} = 0.9$ GHz width. 10000 spectra of randomly oriented complexes were accumulated. The hole is shown against the relative energy where $\Delta E°$ denotes the shift of transition a when $g_x = g_y = g_z = 2.17$. (a) The effect of *g*-strain with $g_x^o = g_y^o = g_z^o = 2.17$, $\sigma_x = \sigma_y = \sigma_z = \sigma$ for various values of the standard deviation σ as indicated. The values for $g_x = g_y = g_z$ were generated by a random Gaussian number generator. (b) The effect of anisotropy with $g_x = 1.9$, $g_y = 2.19$, and $g_z = 2.4$ in trace o and $g_x = 1.8$, $g_y = 2.18$, and $g_z = 2.5$ in trace p. Trace i shows again the case with no anisotropy or *g*-strain.

The original hole depth in the experiment of Figure 5 is ≈15%. The relative hole contributions are thus approximately proportional to the square of the Boltzmann populations of the ground-state spin levels, $P(M_S')^2$, and the transitions d, e, and f can be neglected. Furthermore, holes due to the transitions b and c are expected to be only about $^1/_7$ of the hole caused by transition a. The hole due to species which have transition b in resonance with the laser is expected to show a minimal shift when varying the external magnetic field. Within the experimental accuracy, limited by the signal-to-noise ratio, no hole can be detected at $\Delta E \cong 0$. We note here that in addition to the Boltzmann factor the geometry of the experiment $\mathbf{E}\perp\mathbf{B}$ is also important. For $\Delta M_S = 0$ transitions between spin-only levels the main polarization is usually $\mathbf{E}||\mathbf{B}$. Hence transition b may be very weak in the present geometry.

The shift of transition c is close to the shift of transition a for *g*-values of the excited state of ≈2. A better signal-to-noise ratio and higher resolution would be needed to detect the hole due to c. We conclude that the major component of the hole in Figure 5 is due to the transition a and by using eq 8 an average excited *g*-value of $g_{ex}^{av} = 2.17$ is evaluated from the 26.4 GHz/T shift.

The broadening of the hole reflects the anisotropy and/or the strain of the **g**-tensor in the excited state. The hole width is ≈1.9 GHz at 2.8 and 3.6 T in comparison with the value of 0.9 GHz at 3.2 T. The simulations shown in Figure 7 provide some semiquantitative analysis of the anisotropy and/or strain of the excited state *g*-value. Figure 7a illustrates the effect of *g*-strain on the width of a hole burned in 3.2 T when the field is changed by 0.38 T. The simulations are the result of accumulating the theoretical spectra of 10000 randomly oriented complexes with equal average values and equal standard deviations σ for g_x^o, g_y^o and g_z^o. The distributions of g_x, g_y, and g_z were created by using a random Gaussian number generator. If the hole broadening in Figure 5 is entirely due to *g*-strain, we can conclude that the standard deviation of the *g*-value of the excited state is about 0.2 or 10%.

Figure 7b shows the effect of anisotropy of the *g*-value on the width of the hole burned in a field of 3.2 T when the magnetic field is varied by 0.38 T. The simulations were performed in the same way as outlined for Figure 7a but with fixed values for g_x, g_y, and g_z. If the hole broadening observed in the experiments of Figure 5 are entirely due to anisotropy, we can conclude that it is of the order of ≈15%. The actual broadening is the product of both *g*-strain and anisotropy.

Nitrogen-bonded thiocyanate-metal complexes often display a metal−N−C bond angle in the range of 160−180° and the N−C−S angle is usually close to 180°. This applies also to chromium(III) complexes and Cr−N−C and N−C−S angles of 164.3° and 176.6°, respectively, were found in crystals of $[Ho(C_6H_4NCO_2H)(H_2O)_2][Cr(NCS)_6]$.[18] It follows then that the $[Cr(NCS)_6]^{3-}$ molecular anion would assume trigonal symmetry in free space due to the repulsion of the ligands. However, the trigonal potential is shallow because of the blunt Cr−N−C angle and in condensed phases minor interactions with host molecules will lower the symmetry. For example, the NCS^- ligand can assume different rotational orientations with respect to the Cr−N axis due to host−guest interactions. Furthermore, the angle Cr−N−C is subject to variations caused by these interactions. The average splitting of the ^2E state of 40 cm^{-1}, and the large variation of this splitting is a direct consequence of the distribution of low symmetry fields which are imposed on the intrinsically trigonal molecular anion. Hence, it is not surprising that the excited state *g*-value is close to spin-only and shows low anisotropy and *g*-strain of the order of magnitude of ≈15%. If the $[Cr(NCS)_6]^{3-}$ species retained its intrinsic trigonal symmetry the *g*-value of the excited state would be highly anisotropic with an effective $g\perp c = 0$ for the R_1 level. The small anisotropy implies that lower symmetry perturbations are dominant and the value $g_{ex}^{av} = 2.17$ (>2.0) indicates that the perturbed R_1 level arises from the trigonal $\bar{E}$ component of the ^2E multiplet. The effect of low symmetry perturbations on a trigonal species has been analyzed previously for $[Cr(2,2'\text{-bipyridine})_3]^{3+}$ embedded in amorphous hosts.[11,15] However, in the present system the trigonal potential is anticipated to be much shallower.

The linear shift observed upon the variation of the external magnetic field when a hole is initially burned in a high field can be used to scan the spectral hole with the laser kept at constant frequency.

This is illustrated in Figure 8 which displays two sweeps of the magnetic field corresponding to frequency changes of 2.38 and 4.49 GHz, respectively.

As is usually observed the hole width is dependent on its depth.[19] The 6% hole implies an upper limit of the homogeneous line width of 300 MHz. This is still 7 orders of magnitude larger than the lifetime limit $\Gamma_{hom} = 1/2\pi T_1$ of ≈30 Hz. Efficient spectral diffusion on the time scale of the experiment is most likely responsible for the major contribution to the observed width.[8] The contribution from R_2 can be neglected on this scale of resolution since the $R_2 \rightarrow R_1$ relaxation rate is expected to correspond to a line width of >5 GHz.[17]

4. Conclusions

The present paper shows that Zeeman measurements on spectral holes in amorphous systems may be very informative if the hole is burned in high magnetic fields. For example, it is

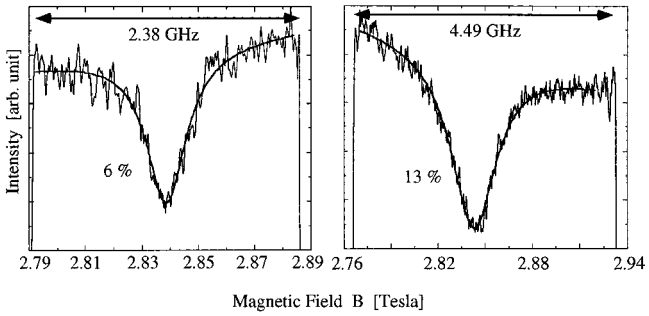

Figure 8. Zeeman scanning of persistent spectral holes in the $[Cr(NCS)_6]^{3-}$/glycerol system at 4.2 K. A spectral hole was burned at 781.81 nm and in a magnetic field of B = 2.84 T for 30 and 80 s, respectively, with a power density of ≈200 mW/cm^2. The hole was read out by sweeping the magnetic field from ≈2.79 to ≈2.88 and ≈2.77 to ≈2.93 T. The field sweeps correspond to 2.38 and 4.49 GHz. For the read out the laser intensity was attenuated by a factor of ≈5.

possible to measure *g*-values and their anisotropies and/or strains for the excited state in specific systems.

Zeeman scanning of spectral holes has been demonstrated previously in crystalline systems.[20] However, it appears that the present paper is the first report of this phenomenon in *amorphous systems*. The Zeeman scanning is possible because spectral holes in particular systems may display a linear shift if burned in a high field. The Zeeman scanning facilitates the measurement of fine details of the electronic structure of molecules and ions in amorphous system. It may also be applied to monitor the drift of laser frequencies over an extended period of time and the homogeneity of magnetic fields if an amorphous system with a very narrow hole width (<10 MHz) is used.

Acknowledgment. Drs L. Dubicki, B. Freasier, L. Wallace, and E. Krausz are acknowledged for their interest in this work and for valuable suggestions and discussions.

References and Notes

(1) Moerner, W. E., Ed. *Persistent Spectral Hole-Burning: Science and Applications*; Topics in Current Physics 44; Springer-Verlag: Heidelberg, 1988.
(2) Völker, S. *Annu. Rev. Phys. Chem.* **1989**, *40*, 499.
(3) Yen, W.; Selzer, P. M., Eds. *Laser Spectroscopy of Solids, Topics in Applied Physics 49*; Springer-Verlag: Berlin, 1981; Vol 49.
(4) Riesen, H.; Krausz, E. *Comm. Inorg. Chem.* **1993**, *14*, 323.
(5) Riesen, H.; Krausz, E. *Chem. Phys. Lett.* **1991**, *182*, 266.
(6) Kharlamov, B. M.; Bykovskaya, L. A.; Personov, R. I. *Chem. Phys. Lett.* **1977**, *50*, 407.
(7) Milanovich, N.; Suh, M.; Jankowiak, R.; Small, G. J.; Hayes, J. M. *J. Phys. Chem.* **1996**, *100*, 9181.
(8) Wannemacher, R.; Koedijk, J. M. A.; Völker, S. *Chem. Phys. Lett.* **1993**, *206*, 1.
(9) Vauthey, E.; Holliday, K.; Wei, C.; Renn, A.; Wild, U. P. *Chem. Phys.* **1993**, *171*, 253.
(10) Reddy, N. R. S.; Small, G. J.; Seibert, M.; Picorel, R. *Chem. Phys. Lett.* **1991**, *181*, 391.
(11) Riesen, H.; Krausz, E.; Dubicki, L. *Chem. Phys. Lett.* **1994**, *218*, 579.
(12) Ferguson, J. In *Electronic States of Inorganic Compounds: New Experimental Techniques*; Day, P., Ed.; Reidel: Dordrecht, 1975; p 59.
(13) Flint, C. D.; Matthews, A. P. *J. Chem. Soc., Faraday Trans. 2* **1974**, *70*, 1301.
(14) Poupko, R.; Baram, A.; Luz, Z. *Mol. Phys.* **1974**, *27*, 1345.
(15) Riesen, H.; Krausz, E.; *J. Chem. Phys.* **1992**, *97*, 7902.
(16) Kador, L.; Schulte, G.; Haarer, D. *J. Phys. Chem.* **1986**, *90*, 1264.
(17) Riesen, H. *J. Lumin.* **1992**, *54*, 71.
(18) Norbury, A. *Adv. Inorg. Chem. Radiochem.* **1975**, *17*, 231.
(19) Van den Berg, R.; Völker, S. *Chem. Phys.* **1988**, *128*, 257.
(20) Wang, Y. P.; Landau, D. P.; Meltzer, R. S.; Macfarlane, R. M. *J. Opt. Soc. Am. B* **1992**, *9*, 946.